Effects of Initial Conditions and Parameters on the Prediction of SARS-CoV-2 Viral Load in the Upper Respiratory Tract Based on Host-Cell Dynamics

Li, Hanyu
Interdisciplinary Graduate School of Engineering Sciences, Kyushu University

Kuga, Kazuki
Faculty of Engineering Sciences, Kyushu University

Nguyen Dang Khoa
Interdisciplinary Graduate School of Engineering Sciences, Kyushu University

Ito, Kazuhide
Faculty of Engineering Sciences, Kyushu University

https://doi.org/10.5109/4738582

出版情報：Proceedings of International Exchange and Innovation Conference on Engineering & Sciences (IEICES). 7, pp.155-160, 2021-10-21. Interdisciplinary Graduate School of Engineering Sciences, Kyushu University
バージョン：
権利関係：

Effects of Initial Conditions and Parameters on the Prediction of SARS-CoV-2 Viral Load in the Upper Respiratory Tract Based on Host-Cell Dynamics

Hanyu Li[1*], Kazuki Kuga[2], Nguyen Dang Khoa[1], Kazuhide Ito[2]
[1] Interdisciplinary Graduate School of Engineering Sciences, Kyushu University, Japan
[2] Faculty of Engineering Sciences, Kyushu University, Japan
[*]Corresponding author email: li.hanyu.296@s.kyushu-u.ac.jp

Abstract: *This study focuses on the deposition of severe acute respiratory syndrome coronavirus 2 (SARS-CoV-2)-laden droplets in the upper respiratory tract of the human body based on host-cell dynamics (HCD). First, the deposition of five particle sizes in the airway was preliminarily obtained by combining and analyzing the results of computational fluid dynamics (CFD) previously studied, and the target cell-limited model was used to roughly predict the variation trend of viral load over time after infection. Then, the initial conditions and parameters in the target cell-limited model were changed to observe the effects on the prediction of viral load. The results showed that the virus-carrying droplets were mainly concentrated in the nasal cavity and throat. The initial susceptible target cells T(0) and other parameters had different effects on the prediction of viral load. Therefore, it is necessary to identify suitable parameters for the dynamic calculation of SARS-CoV-2.*

Keywords: SARS-CoV-2, Upper respiratory tract, Host-cell dynamics, Initial conditions, Parameters

1. INTRODUCTION

In December 2019, the sudden outbreak of coronavirus disease 2019 (COVID-19) engulfed almost the entire world and was caused by a novel coronavirus named severe acute respiratory syndrome coronavirus 2 (SARS-CoV-2) approximately 0.1μm in diameter [1,2]. With the expansion of COVID-19, several scholars have carried out extensive clinical case data research and discussion on the transmission and pathogenesis. Aerosol transmission is an important mechanism of infection. It occurs when a patient sneezes and cough droplets carrying the virus are disseminated. Larger droplets settle naturally, while others can suspend in the air for a long time [3]. Therefore, several studies have focused on the deposition of viral droplets in the respiratory tract.

Kim et al. [4] presented the different viral load dynamics of the first two confirmed Korean patients with mild to moderate disease, and suggested that the viral load dynamics of SARS-CoV-2 may differ from those of other previously reported coronavirus infections, such as SARS-CoV. Prentiss et al. [3] used five well-documented case studies and a simple physical model of airborne transmission to estimate the characteristic number of SARS-CoV-2 required to induce infection in each case and provided a basis for estimating the risk of daily activities. Wölfel et al. [5] reported a detailed virological analysis of nine cases and confirmed the active replication of the virus in the larynx, providing evidence for active replication in the upper respiratory tract tissue, which is of great significance for the prevention of infection. Fatehi et al. [6] introduced a COVID-19 intracellular dynamics model based on random subjects. The predictions were combined with an intercellular model of intra-host infection dynamics to fit the clinical data in a previous study [5] to generate a general profile of disease progression in patients who recovered in the absence of treatment. Hernandez-Vargas et al. [7] studied the human-host mathematical model of COVID-19. According to the target cell-limited model, the number of viral replicas of SARS-CoV-2 in the host was consistent with the broad value of human influenza infection.

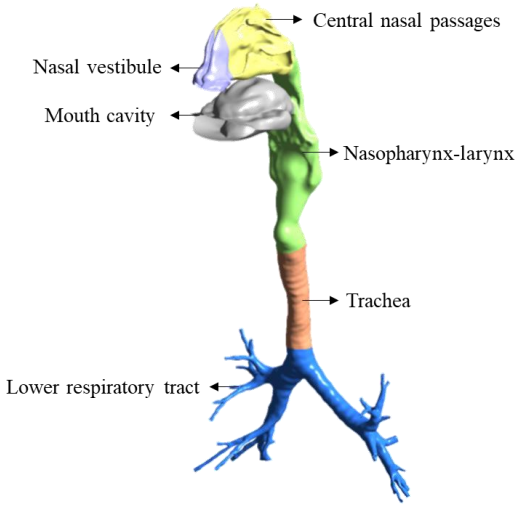

Fig. 1. A 3-dimensional model of the human respiratory tract

Furthermore, the sophisticated model with consideration of immune cell responses suggested that a slow immune response peaked 5 to 10 days after symptom onset.

SARS-CoV-2 can be transmitted through droplets in the respiratory tract. Therefore, to understand the deposition of SARS-laden droplets in the human upper respiratory tract, computational fluid dynamics (CFD) simulations were performed. CFD is often selected to simulate the flow, particle, and temperature fields, among others. For example, in previous conference papers [8,9] of IEICES, this method was used to simulate the changes in blood flow and heat exchange of the heat pump. For different cases, different CFD models were selected for simulation, and the results were relatively reliable and could withstand verification. The host-cell dynamics (HCD) model refers to the mathematical models of viral dynamics in the host that consider the interactions among target cells, the immune system, and viral agents. It was developed independently from existing studies and can be used to calculate changes in viral load and target cell number, among others [10].

As mentioned above, SARS-CoV-2 can actively replicate in the upper respiratory tract. Changes in the viral load

can also cause symptomatic reactions in patients. Hence, CFD and HCD were combined to study the deposition of airborne virus-laden droplets and to predict the viral load in the upper respiratory tract under nasal inhalation conditions. In addition, the initial conditions were changed to observe the effects of various parameters on the predicted results of viral load.

2. METHODS

As shown in Fig. 1, this study was based on a 3D respiratory tract model created from an Asian healthy volunteer. The respiratory tract model was divided into six parts, namely the nasal vestibule, central nasal passage, nasopharynx-larynx, trachea, mouth cavity, and lower respiratory tract. The latter two were not considered in this study.

Assuming the worst case scenario that there is a healthy person with a breathing rate of 7.5 L/min (gentle breathing state) in a close conversation with an infected person, and 10,000 droplets coughed up by the infected person are directly inhaled by the other person through nasal inhalation.

With regards to two previous studies, Fig. 2 shows the number concentration plotted based on the size distribution of droplets released when people cough [11,12]. More than 70% of the droplets were less than 10 μm in diameter.

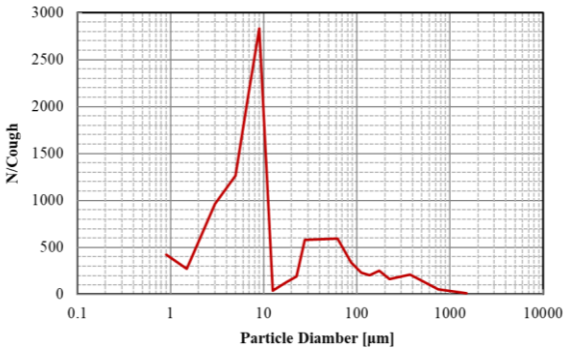

Fig. 2. Size distribution of droplets when coughing

Table 1 Basic initial conditions for the HCD model

Basic Conditions		Value
Surface area (m^2)		3.38E-02
V_{mucus} (mL)		0.51
T(0) [cells]		8.46E+08
Particles	1 μm	14
	2.5 μm	28
	5 μm	46
	7.5 μm	163
	10 μm	243
Percentage		4.94%
V(0) [copies/mL]		1.66E-02

Consistent with the previous study, five particle sizes (1, 2.5, 5, 7.5, and 10 μm) were selected as representatives for the CFD calculation [13]. The total deposition results were calculated according to the proportion in Fig.2, as shown in Table 1.

The HCD of SARS-CoV-2 was preliminarily calculated using the target cell-limited model, which has been previously verified to fit the trend of clinical data change well and is represented by the following equations [7]:

$$\frac{dT(t)}{dt} = -\beta T(t)V(t) \quad (1)$$

$$\frac{dI(t)}{dt} = \beta T(t)V(t) - \delta I(t) \quad (2)$$

$$\frac{dV(t)}{dt} = \frac{p'}{V_{mucus}} I(t) - cV(t) \quad (3)$$

where T, I, and V represent the number of susceptible target cells, infected cells, and viral load, respectively. Initially, the variation of viral load in different parts was calculated using parameters from a previous study. Assuming that the infection occurred 3 days before symptom onset, the target cells were infected at the rate $\beta = 4.71 \times 10^{-8}$ (copies/mL)day^{-1} and apoptosis of infected cells occurred at $\delta = 1.07$ day^{-1}. The virus clearance rate is $c = 2.4$ day^{-1} [7]. Equation (3) was been modified slightly, so that instead of using a uniform rate p of virus production [(copies/mL)/day/cell], the rate of virus production in each part of the respiratory tract is calculated separately, making the results closer to the actual situation. Therefore, the virus production rate was set as $p' = 0.74$ copies/day/cell, and the volume of mucus (V_{mucus}) was calculated as the product of surface area (see Table 2) and thickness (15 μm) [14].

Table 2 Geometric parameters of different regions

Regions	Surface area (m^2)	V_{mucus} (mL)
Vestibule	3.71E-03	0.06
Central nasal passages	1.55E-02	0.23
Nasopharynx-larynx	9.88E-03	0.15
Trachea	4.72E-03	0.07
Total	3.38E-02	0.51

The initial number of target cells, $T(0)$, was estimated according to the total surface area of the airway and the surface area of each epithelial cell, which was assumed to be 4×10^{-11} m^2/cell [15]. Meanwhile, the initial virus load, $V(0)$, was calculated based on droplet sizes and the percentage of deposition, as well as the amount of virus carried in each droplet, which depended largely on the patients and infection status and was assumed to be 10^5 copies/mL.

Due to the limited clinical data currently available, studies are greatly varied, such as in terms of the parameters of the initial condition. Therefore, the present study also substituted the initial conditions and parameter values in different studies into the model calculation in an attempt to determine the influence of each parameter on the change in viral load.

In the calculation, when the parameters ($T(0)$, $V(0)$, β, δ, c, p', and V_{mucus}) changed separately and successively, other conditions should be kept consistent. These values are listed in Table 3. Other values without superscripts and special instructions were selected at random for comparison.

3. RESULTS AND DISCUSSION

The main results of CFD and HCD calculations concerning the deposition of SARS-CoV-2-laden droplets in the human upper respiratory tract and the effects of initial conditions and parameters on the prediction of viral load by the host-cell dynamics model are presented in detail in the following sections.

3.1 Deposition of SARS-CoV-2 Laden Droplets in the Upper Respiratory Tract

The deposition of SARS-CoV-2-laden droplets is shown in Fig.3. This result was obtained by scaling and simply adding up the deposition data for five particle sizes.

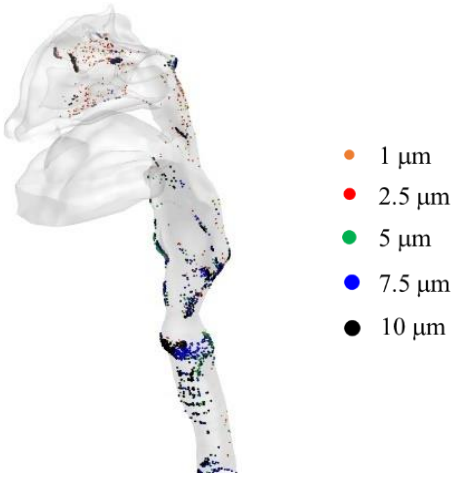

Fig. 3. Deposition of droplets with different sizes

The droplets were mostly concentrated around the nasal cavity and throat, which might explain the stuffy nose and sore throat. As can be seen from the percentage of particles deposited in Table 1, most of the fine particles entering the lower part may cause severe symptoms.

In Fig.4, the peak value of the viral load is more than 10^8 copies/mL, which is also consistent with the range of the peak value of viral load (10^6–10^9 copies/mL) in the clinical data of patients who were in the early stages of COVID-19 symptoms [5]. Furthermore, the viral load peaked around 5 days after infection and decayed below the detection limit at approximately 18 days after infection.

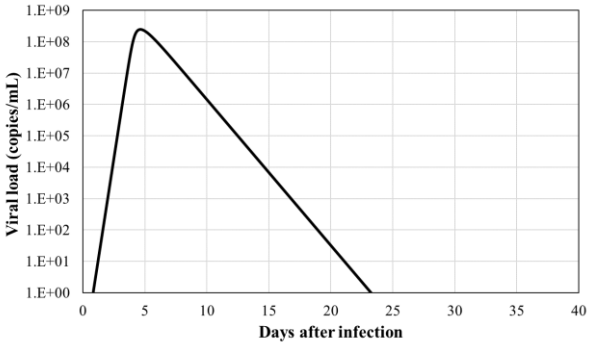

Fig. 4. Viral load over time

3.2 Effects of initial conditions and parameters on prediction of viral load

In Equations (1)–(3), the other initial conditions and parameter values were kept unchanged, and the changes in $T(0)$, $V(0)$, β, δ, c, p', and V_{mucus} are listed in Table 3. The results are presented Fig.5.

As shown in Fig.5 (a), $T(0)$ can strongly affect the viral dynamics not only in the viral peak load, but also in the duration when the virus can be detected. The larger the $T(0)$ is, the faster the virus load increases and the higher the peak it can reach, which can be detected rapidly in the early stages of infection.

Table 3 Changes in initial condition parameters

Parameters to be changed	1	2	3	4	5	6
T(0) [cells]	1.0E8	4.0E8 [a]	8.46E8 [b]	1.0E9 [c]	1.0E10 [c]	1.0E11 [c]
V(0) [copies/mL]	0.001	0.0166 [b]	0.031 [d]	0.1 [e]	1.0	\
β [(copies/mL) day^{-1}]	1.58E-8 [d]	2.54E-8 [e]	4.71E-8 [b d]	1.11E-7 [e]	2.07E-7 [e]	\
δ [day^{-1}]	0.17 [e]	0.265 [e]	0.51 [e]	1.04 [d]	1.07 [b d]	\
c [day^{-1}]	0.75 [e]	1.75 [e]	2.4 [b d]	3.91 [e]	\	\
p' [copies/day/cell]	0.2	0.5	0.74 [b d]	1.3	2.0	\
V_{mucus} [mL]	0.1	0.39 [f]	0.51 [b f]	1.0	2.0	\

Annotation:
a Baccam et al., 2006 [16]
b Values used in the present study.
c Bar-On YM et al., 2020 [17]
d Esteban A. Hernandez-Vargas et al., 2020 [7]
e Fatehi, F.et al., 2020 [6]
f Calculated values according to Phuong NL et al., 2020 [13]

Conversely, $V(0)$ had little effect on the change. As shown in Fig.5(b), it did not affect the peak viral load. Only when it is small, it will delay the detection of virus. Fig.5(c) shows that the value of the cell infection rate, β, has little effect on the peak viral load as well as the effect of $V(0)$. However, it varies by an order of magnitude and has a slightly greater impact on the time to detect the virus than $V(0)$. The larger the β, the faster the target cell becomes infected, the faster the viral load increases, and the sooner it can be detected.

Furthermore, Fig.5(d) shows that the influence of the mortality rate of infected cells, δ, on viral dynamics is mainly concentrated at the later stage of infection. The lower the value of δ, the slower the apoptotic rate of the

infected cells, and the more likely it is to infect more target cells, resulting in prolonged illness and severe symptoms.

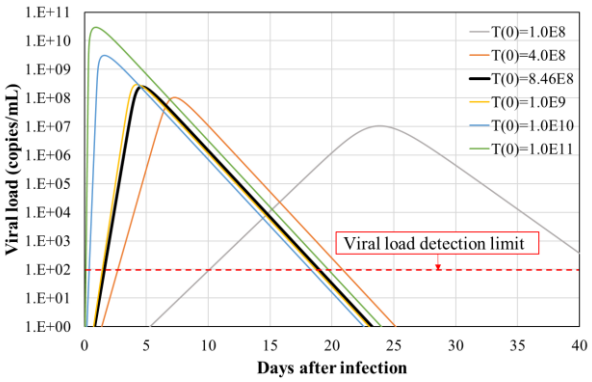

(a)

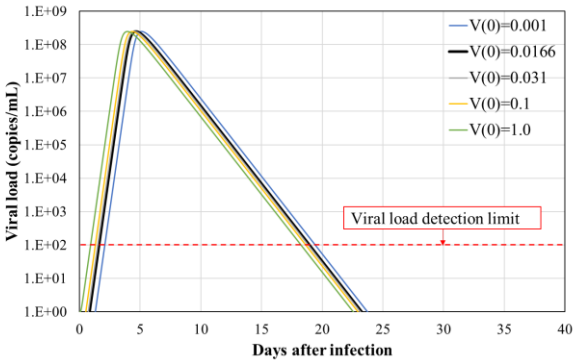

(b)

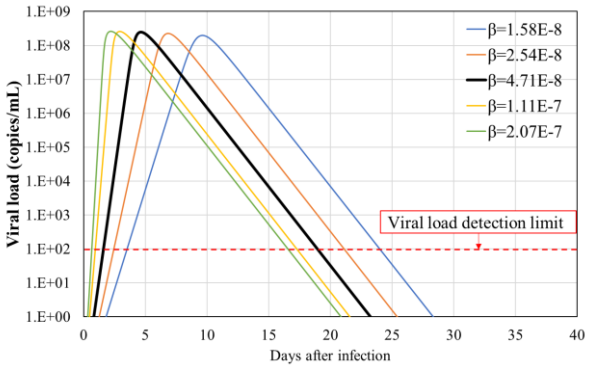

(c)

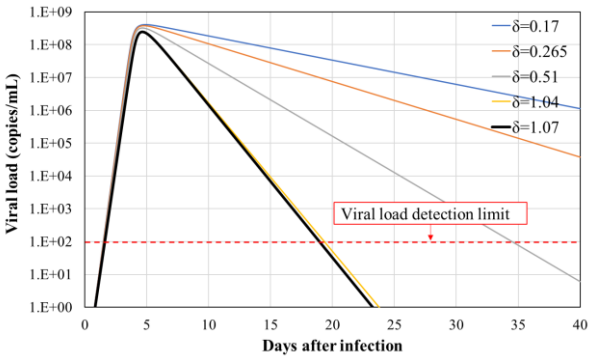

(d)

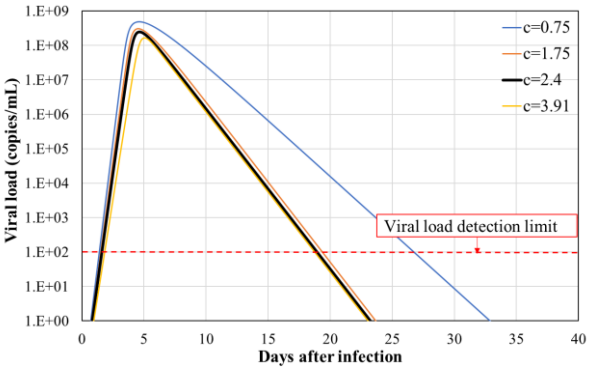

(e)

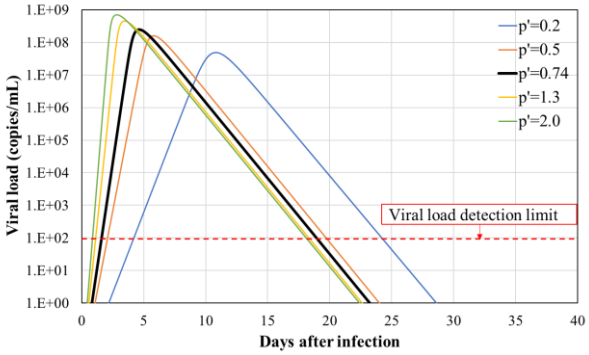

(f)

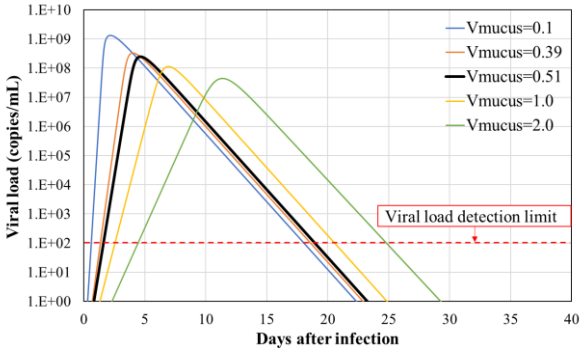

(g)

Fig. 5. Trend of viral load prediction under different parameter values (The black bold lines are the data used in the present study)

There was little difference in the virus clearance values in literature. Fig.5(e) shows that the virus clearance rate, c, has a certain degree of influence on the growth rate and peak value of virus, and the self-healing time of patients. Accelerating the virus clearance rate can inhibit the growth of the virus to a certain extent and shorten the self-healing time.

As shown in Fig. 5(f) and (g), since $I(0)$ and $V(0)$ almost approached zero, the early increase in their number was mainly regulated by the number of target cells, and the changes in δ and c mainly affected the process of viral load reduction. Nevertheless, it seems that δ has a greater effect on the result than c by changing the order of magnitude. To analyze possible causes, a medical book [18] noted that the virus is destroyed because human innate (e.g., natural killer cells) and adaptive immunity (e.g., T cells) drive host cells to die before replication is complete. Therefore, when the death rate of infected cells,

δ, increases, the replication and clearance mechanisms of the virus in these cells are broken down, which has a greater impact on viral load changes than just an increase in virus clearance, c.

Combining Fig.5(f) and (g), it can be seen that for the same V_{mucus}, the faster the virus production rate p' is, the faster it reaches the peak of viral load, and the higher its peak is. Nevertheless, the value of p' has little effect on the length of time over which the virus can be detected. When the rate of virus production p' is constant, the more the mucus, the smaller the number of viruses produced per unit volume of mucus. With all other factors being equal, the less the mucus, the more serious the infection is likely to be.

In this study, the most basic model was only used to calculate and try to determine the influence of various initial conditions and parameters on the load change of SARS-CoV-2, ignoring the immune system's response to the virus and how the virus spreads, replicates itself, and infects cells in the mucus layer of the respiratory tract. This still needs to be investigated in future research. Moreover, HCD and CFD can be combined in a deeper way. Laden droplets with mixed particle sizes can be used as the initial conditions for transient calculations, and the regional deposition of SARS-CoV-2-laden droplets in the upper respiratory tract can be simulated.

4. CONCLUSIONS

In this study, CFD and HCD were used for the simple simulation and calculation of droplet deposition at different parts of the upper respiratory tract. The effects of initial conditions and various parameters on the trend prediction of viral load were calculated and discussed according to the target cell-limited model. The conclusions are as follows:

The SARS-CoV-2-laden droplets mostly collected in the nasal cavity and throat, which may be the cause of inflammatory response.

For the prediction of the viral load, the trend of the viral dynamics was shown under the calculation conditions set in this study.

For the effects of the initial conditions and parameters within the HCD model, the impact of $T(0)$ is strong for the viral dynamics, especially at the peak value of the virus load, while $V(0)$ and β mainly affect the time when the virus is detected. The changes in δ and c have an obvious effect on the degree of virus attenuation. To a certain extent, c inhibited the growth rate of the virus. Moreover, p' and V_{mucus} primarily affect the rate of virus production per unit volume of mucus, and the higher their value, the more severe the disease is likely to be.

Taken together, these results may contribute to the understanding of early recognition of infection and the importance of selecting accurate initial conditions and parameters for viral load calculation and prediction of SARS-CoV-2. This is essential to further understand and predict the COVID-19 condition in patients.

5.REFERENCES

[1] C.C. Lai, T.P. Shih, W.C. Ko, H.J. Tang, and P.R. Hsueh. Severe acute respiratory syndrome coronavirus 2 (SARS-CoV-2) and corona virus disease-2019 (COVID-19): the epidemic and the challenges. Int. J. Antimicrob. Agents, page 105924, 2020.

[2] Bar-On YM, Flamholz A, Phillips R, Milo R. SARS-CoV-2 (COVID-19) by the numbers. Elife. 2020;9: e57309. Published 2020 Apr 2. doi:10.7554/eLife.57309

[3] Mara Prentiss, Arthur Chu, Karl K. Berggren. Superspreading Events Without Superspreaders: Using High Attack Rate Events to Estimate Nº for Airborne Transmission of COVID-19, medRxiv 2020.10.21.20216895; doi: https://doi.org/10.1101/2020.10.21.20216895

[4] Kim JY, Ko JH, Kim Y, Kim YJ, Kim JM, Chung YS, Kim HM, Han MG, Kim SY, Chin BS. Viral Load Kinetics of SARS-CoV-2 Infection in First Two Patients in Korea. J Korean Med Sci. 2020 Feb 24;35(7):e86. doi: 10.3346/jkms.2020.35.e86. PMID: 32080991; PMCID: PMC7036338.

[5] Wölfel, R., Corman, V. M., Guggemos, W., Seilmaier, M., Zange, S., Müller, M. A.Wendtner, C. (2020). Virological assessment of hospitalized patients with COVID-2019.Nature,1–10. https://doi.org/10.1038/s41586-020-2196-x

[6] Fatehi, F., Bingham, R. J., Dykeman, E. C., Stockley, P. G., and Twarock, R., Comparing antiviral strategies against COVID-19 via multi-scale within host modelling, 2020. arXiv:2010.08957

[7] Esteban A. Hernandez-Vargas, Jorge X. Velasco-Hernandez, In-host Mathematical Modelling of COVID-19 in Humans, Annual Reviews in Control, Volume 50, 2020, Pages 448-456, ISSN 1367-5788, https://doi.org/10.1016/j.arcontrol.2020.09.006.

[8] Haghnegahdar A, Zhao J, Feng Y. Lung Aerosol Dynamics of Airborne Influenza A Virus-Laden Droplets and the Resultant Immune System Responses: An In Silico Study. J Aerosol Sci. 2019 Aug;134:34-55. doi: 10.1016/j.jaerosci.2019.04.009. Epub 2019 Apr 24. PMID: 31983771; PMCID: PMC6980466.

[9] Shamudra Dey, Tahsin Ibtida, Chandan Kumar Roy, Nuruzzaman Sakib. Difference between Non-Newtonian Carreau and Casson Blood Viscosity Models to Predict Hemodynamics in Idealized Eccentric Arterial Stenosis: Large Eddy Simulation Modeling, 2020. Proceedings of International Exchange and Innovation Conference on Engineering & Sciences (IEICES), vol6:249-257, https://doi.org/10.5109/4102499

[10] Muhammad Tahir Jamil, Yong Hai Yu, Fiaz Ahmad, Applications of Different Turbulence Models in CFD Simulations of Mixed Flow Hydraulic Pump, 2020. Proceedings of International Exchange and Innovation Conference on Engineering & Sciences (IEICES), vol6:73-78, https://doi.org/10.5109/4102466

[11] Duguid JP. The size and the duration of air-carriage of respiratory droplets and droplet-nuclei. J Hyg (Lond). 1946;44(6):471-479. doi:10.1017/s0022172400019288

[12] Yang S, Lee GW, Chen CM, Wu CC, Yu KP. The size and concentration of droplets generated by coughing in human subjects. J Aerosol Med. 2007 Winter;20(4):484-94. doi: 10.1089/jam.2007.0610. PMID: 18158720.

[13] Phuong NL, Khoa ND, Ito K. Comparative numerical simulation of inhaled particle dispersion in upper human airway to analyse intersubject

differences. Indoor and Built Environment. 2020;29(6):793-809. doi:10.1177/1420326X19894128

[14] Shang Y, Inthavong K, Tu J. Development of a computational fluid dynamics model for mucociliary clearance in the nasal cavity. Journal of Biomechanics. 2019 Mar;85:74-83. DOI: 10.1016/j.jbiomech.2019.01.015.

[15] Fedoseev G B, Geharev S. Basic defense mechanisms of bronchio-lung system[J]. General pulmonology, 1989, 1: 112-144.

[16] Baccam, P., Beauchemin, C., Macken, C.a., Hayden, F. G., & Perelson, A. S. (2006). Kinetics of influenza A virus infection in humans. Journal of virology, 80(15),7590–7599.

[17] Bar-On YM, Flamholz A, Phillips R, Milo R. SARS-CoV-2 (COVID-19) by the numbers. Elife. 2020 Apr 2;9:e57309. doi: 10.7554/eLife.57309. PMID: 32228860; PMCID: PMC7224694.

[18] Xuetao Cao, Wei He, et, al. Medical Immunology[M]. Beijing: People's Medical Publishing House(PMPH), 2015.